A Model for Human Cytochrome P_{450} 2D6 Based on Homology Modeling and NMR Studies of Substrate Binding†

S. Modi,‡,§,|| M. J. Paine,⊥ M. J. Sutcliffe,# L.-Y. Lian,‡,§ W. U. Primrose,‡,§ C. R. Wolf,⊥ and G. C. K. Roberts*,‡,§,||

Department of Biochemistry, Biological NMR Centre, Centre for Mechanisms of Human Toxicity, and Department of Chemistry, University of Leicester, Leicester LE1 9HN, U.K., and Biomedical Research Centre, Ninewells Hospital and Medical School, University of Dundee, DD1 9SY, Dundee, U.K.

Received November 17, 1995; Revised Manuscript Received January 16, 1996⊗

ABSTRACT: The cytochrome P_{450} responsible for the debrisoquine/sparteine polymorphism (P_{450} 2D6) has been produced in large quantities by expression of a modified cDNA in baculovirus. A polyhistidine extension was incorporated at the C-terminus of the expressed protein, which, after purification of the protein on a nickel-agarose column, could be removed proteolytically by treatment with thrombin. Purified yields of P_{450} 2D6 were 2.4 mg from 700 mL of cell culture. The protein had a greater than 90% heme content and was fully active, having no residual absorbance at 420 nm in the reduced CO complex. The quantities produced allowed direct study of the interaction of the substrate codeine with the enzyme by paramagnetic relaxation effects on the NMR spectrum of the substrate. Distances between the heme iron atom and substrate protons were calculated from these experiments, and the orientation of the substrate in the binding pocket was determined. This showed that codeine was bound with the methoxy group of the molecule closest to the heme iron (iron−methyl proton distance of 3.1 ± 0.1 Å), consistent with the observed O-demethylation to morphine. A model of the complex of P_{450} 2D6 with codeine was built from a multiple sequence and structure alignment of the known crystal structures for P_{450}s, incorporating the experimental constraints derived from the NMR studies. This showed that the overall fold of P_{450} 2D6 is more similar to that of P_{450} BM3 than to either P_{450} *cam* or P_{450} *terp*. Codeine binds to P_{450} 2D6 so that the methoxy group is directly above the A ring of the heme, while the basic nitrogen interacts with the carboxylate of aspartate 301.

The cytochrome P_{450}s[1] constitute a superfamily of heme enzymes that catalyze the monooxygenation of a wide variety of endogenous and xenobiotic compounds through the insertion of one atom of molecular oxygen into the substrate, with the concomitant reduction of the other atom to water. Cytochrome P_{450}s are divided into two classes according to their redox partners: class I cytochrome P_{450}s, found in the mitochondrial membrane of eukaryotes and in bacteria, which are associated with an iron−sulfur protein which mediates electron transfer to the P_{450} from an NADH-dependent FAD- or FMN-containing reductase; and class II enzymes from the endoplasmic reticulum of eukaryotes, which are of most interest in the context of xenobiotic metabolism, and which require only a single redox partner, the flavoprotein NADPH−cytochrome P_{450} reductase.

Cytochrome P_{450} 2D6 (P_{450} 2D6) is a class II enzyme which metabolizes a wide range of compounds containing a basic nitrogen atom. Many of these are of therapeutic interest, including the antihypertensive agent debrisoquine, tricyclic depressants, the morphine-related compounds dextromethorphan and codeine, and a number of others, including bufuralol and perhexiline (Eichelbaum & Gross, 1990). The cDNA encoding human P_{450} 2D6 has been characterized (Gonzalez et al., 1988) and the gene localized to the q13.1 region of chromosome 22 (Gough et al., 1992).

Cytochrome P_{450} 2D6 is responsible for the so-called debrisoquine/sparteine type polymorphism (Lennard, 1990; Meyer et al., 1990) which occurs in 3−10% of the caucasian population. These individuals ("poor metabolizers") have mutations in the CYP2D6 gene [see, e.g., Daly et al. (1995)] which lead to impaired metabolic oxidation of xenobiotics. The clinical relevance of this polymorphism has been established through epidemiological and familial studies (Eichelbaum & Gross, 1990). For example, debrisoquine is extensively metabolized in normal individuals to 4-hydroxydebrisoquine, a major urinary metabolite, but poor metabolizers can develop levels of the parent compound which may be toxic. The impaired metabolic oxidation of at least 30 drugs with diverse structures and pharmacological actions has been associated with the phenotype of poor debrisoquine metabolism. Poor metabolizers may additionally be unable to bioactivate a parent drug such as encainide to its therapeutically active metabolites. It would be of considerable value, both in the design of new therapeutic compounds and in the understanding of environmental toxins, to be able

† This work was supported by a grant from the Medical Research Council. The Leicester Biological NMR Centre is supported by the Biotechnology and Biological Sciences Research Council. M.J.S. is a Royal Society University Research Fellow.

* Address correspondence to this author at Centre for Mechanisms of Human Toxicity, University of Leicester, P.O. Box 138, Hodgkin Building, Lancaster Road, Leicester LE1 9HN, U.K. Telephone: +44-(0)116-252-5534. Fax: +44-(0)116-252-5526/5616.

‡ Department of Biochemistry, University of Leicester.

§ Biological NMR Centre, University of Leicester.

|| Centre for Mechanisms of Human Toxicity, University of Leicester.

⊥ University of Dundee.

Department of Chemistry, University of Leicester.

⊗ Abstract published in *Advance ACS Abstracts,* March 15, 1996.

[1] Abbreviations: P450, cytochrome P_{450}; P_{450} 2D6, human cytochrome P_{450} 2D6; P_{450} BM3, cytochrome P_{450} BM3 from *B. megaterium*; PCR, polymerase chain reaction; PMSF, phenylmethanesulfonyl flouride; DTT, dithiothreitol.

0006-2960/96/0435-4540$12.00/0

to predict the metabolic fate of any xenobiotic with P_{450} 2D6 (and other cytochrome P_{450}s) and the effect that polymorphism in this gene might have on the extent and character of the metabolism. To this end, structural information on the active site of P_{450} 2D6 is required.

A number of high-resolution structures of cytochromes P_{450} have been determined. These include cytochrome P_{450} *cam* (CYP101) from *Pseudomonas putida*, which catalyzes the 5-*exo*-hydroxylation of camphor (Poulos et al., 1986, 1987; Poulos & Raag, 1992; Raag et al., 1991, 1993, and references therein), cytochrome P_{450} BM3 (CYP102) from *Bacillus megaterium*, which catalyzes the hydroxylation of saturated and monounsaturated fatty acids, alcohols, and amides at the ω-1, ω-2, and ω-3 positions (Ravichandran et al., 1993), cytochrome P_{450} *terp* (CYP108) (Hasemann et al., 1994), and cytochrome P_{450} *eryF* (Cupp-Vickery & Poulos, 1995). Studies of these crystal structures have provided valuable insight into the mechanism of cytochrome P_{450}s [e.g., Poulos et al. (1987), Raag et al. (1991), Poulos and Raag (1992), Loida and Sligar (1993), Ravichandran et al. (1993), and Hasemann et al. (1995)]. However, of these enzymes only P_{450} BM3 is a class II enzyme, similar to those of the mammalian endoplasmic reticulum. There is no direct structural information on any of the latter enzymes, and a number of attempts have been made to build models of their structures by homology modeling based on the crystal structure of P_{450} *cam* and knowledge of the range of substrates of each enzyme [e.g., for P_{450} 2D6, Ferenczy and Morris (1989), Zvelebil et al. (1991), Islam et al. (1991), and Koymans et al. (1992, 1993)]. The overall homology between P_{450} 2D6 and P_{450} cam, however, is low. More recently, models have been built on the basis of the structure of the more closely related P_{450} BM3 (Lewis, 1995). However, the wide variation in substrate specificity between different members of the P_{450} superfamily makes it difficult to generate models of the active site sufficiently accurate to allow predictions of the metabolic fate of xenobiotics. To improve the accuracy of the models and to allow them to be tested, experimental structural information on the active site is required. We have recently shown that measurements of paramagnetic relaxation can be used to determine distances between the heme iron and protons of the bound substrate and hence to build a model of the enzyme−substrate complex (Modi et al., 1995a).

In the present study, we report the expression of P_{450} 2D6 in baculovirus, its purification in sufficient quantities for NMR studies, and the construction of a model for the enzyme−substrate complex by combining modeling of P_{450} 2D6 from a multiple sequence and structure alignment of all the available crystal structures for P_{450}s with the results of the NMR experiments, thus improving the accuracy of the modeling of the active site.

MATERIALS AND METHODS

Materials. His-Bind resin was obtained from Novagen; PD10 and Mono Q (5/5) FPLC columns were obtained from Pharmacia. All media were obtained from GIBCO. Codeine, bufuralol, and thrombin were obtained from Sigma; all other chemicals used were of at least analytical grade.

Baculovirus Constructs. The cytochrome P_{450} 2D6 for the NMR experiments was obtained by using a modification of the baculovirus expression system described recently (Paine et al., 1996). The cDNA encoding the full length wild-type

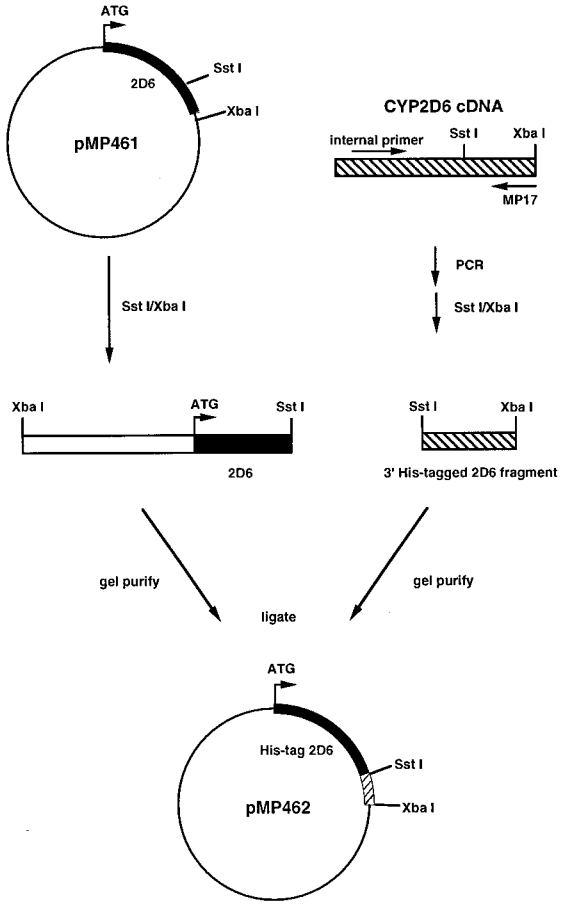

FIGURE 1: Construction of C-terminally His-tagged CYP2D6. A 973 bp fragment of CYP2D6 was amplified by PCR using oligonucleotide MP17 (see text) and an internal CYP2D6 primer (5′-ACGTGATCGGCCTCCCTCAC). A 166 bp 3′ modified DNA fragment was generated from this by *Sst*I/*Xba*I digestion and used to replace the corresponding sequence in the *Sst*I/*Xba*I excised 3′ region of pMP461. pMP462 contains no additional 3′ noncoding CYP2D6 cDNA, and DNA sequencing was carried out to ensure there were no errors introduced by PCR. The position of the ATG translational start codon in CYP2D6 cDNA is indicated.

coding sequence of CYP2D6 (Kimura et al., 1989) was derived from the plasmid pMP201 constructed previously and used elsewhere for the expression of CYP2D6 in yeast (Ellis et al., 1992). In pMP201 the CYP2D6 cDNA sequence is flanked by *Eco*RI restriction sites and extends from the ATG translation initiation codon to a position 73 bp downstream of the translation termination codon in the 3′ noncoding region. The entire 1567 bp CYP2D6 cDNA sequence was excised from pMP201 with *Eco*RI and ligated into a unique *Eco*RI site adjacent to the promoter P_{cor} in the baculoviral transfer vector pAcMP1 (Pharmingen) to create the transfer plasmid pMP461. Modifications to the 3′ end of the CYP2D6 cDNA to facilitate the purification of the protein were carried out by PCR to create a transfer vector pMP462, as shown in Figure 1. In pMP461, there is a unique *Sst*I site situated near the end of the coding region (1358 bp from the ATG start codon) of CYP2D6 and an *Xba*I site 3′ of the cDNA sequence in the multiple coding site. Therefore, in order to minimize the introduction of PCR errors in CYP2D6, a synthetic oligonucleotide (MP17, 5′-TC**TCTAGA**CTAATGATGATGATGGCTGCCGCGCGGCAC-CAGGCGGG′GCACAGCACAA-3) containing an *Xba*I restriction site (shown in bold) and encoding, respectively, a stop codon, five histidine residues, and a thrombin cleavage site, was used to amplify the region between the natural

translation termination and the unique *Sst*I site. Following *Sst*I/*Xba*I digestion, the resulting 166 bp 3′ modified DNA fragment was used to replace the corresponding region in *Sst*I/*Xba*I digested pMP461. The transfer vector thus constructed (pMP462), encoding a protein containing an 11 amino acid C-terminal extension (LVPRGSHHHHH), was cotransfected with linearized AcRP23.*lacZ* DNA using a BaculoGold expression system (Pharmingen) into Sf9 cells according to the manufacturer's instructions. Thrombin cleavage of the protein expressed by the construct results in a P_{450} 2D6 enzyme with a four amino acid extension (LVPR) relative to the wild-type protein.

Sf9 Cell Culture and Recombinant Protein Expression. Sf9 cells were maintained at 27 °C in TNM-FH media according to standard procedures (O'Reilly et al., 1992). Expression was initiated by infection with baculovirus when suspension cultures were $1.5-2.0 \times 10^6$ cells/mL. Hemin chloride was added to the culture media at 2.5 μg/mL to compensate for the low endogenous levels of heme in insect cells. Cells were harvested 48−72 h after infection, washed once with phosphate buffered saline solution, and stored frozen at −70 °C until use.

Protein Purification. All purification steps were carried out at 4 °C unless stated otherwise. Cells were thawed and suspended in binding buffer (20 mM Tris-HCl, pH 7.9, containing 5 mM imidazole, 2 mM CHAPS, 0.5 M NaCl, 60 μg/mL PMSF, and 20% glycerol). The suspension was sonicated (Sanyo ultrasonic disintegrator Model 150) at highest power (3×10 s, interspersed by 90 s delays) and centrifuged at 35 000 rpm for 1 h (Beckman L7 centrifuge with 50.2Ti rotor), and the supernatant was loaded onto a 5 mL nickel-agarose (His-Bind resin) column (Arnold, 1991). The column was washed with 40 mL of binding buffer and then with 40 mL of 20 mM Tris-HCl, pH 7.9, containing 60 mM imidazole, 0.2 mM CHAPS, 0.5 M NaCl, 60 μg/mL PMSF, and 20% glycerol, to remove weakly bound contaminants. The P_{450} 2D6 protein was eluted with 20 mL of 20 mM Tris-HCl, pH 7.9, containing 1.0 M imidazole, 0.5 M NaCl, 60 μg/mL PMSF, and 20% glycerol. The protein was exchanged into 20 mM Tris-HCl, pH 8.4, 150 mM NaCl, and 2.5 mM $CaCl_2$, using a gel filtration column (PD-10), and the solution was concentrated to 500 μL (Amicon concentrator with 10 kDa cut-off membrane). The His-Tag was removed from the C-terminus of the protein by adding thrombin so that the final ratio of thrombin/P_{450} 2D6 was 1:2000 (w/w) (pET system Manual, 3rd edition, Novagen). The proteolysis reaction was stopped after 2 h by addition of PMSF (60 μg/mL). Any uncleaved P_{450} 2D6 still bearing the C-terminal oligo-His sequence was removed by passing the solution through the nickel-agarose column. The eluent (15 mL) containing P_{450} 2D6 was dialyzed against 2 L of anion exchange buffer (20 mM Tris-HCl, pH 7.5, containing 0.2 mM DTT, 1 mM EDTA, 1 mM benzamidine, and 60 μg/mL PMSF) and loaded onto a Mono Q column. The column was washed with 60 ml of anion exchange buffer, and the P_{450} 2D6 was eluted with a linear salt gradient (0−0.2 M KCl) in the same buffer. Protein concentrations were determined using the Bradford (1976) method with bovine serum albumin solutions as standards. The P_{450} concentration was measured by the method of Omura and Sato (1964) using $\epsilon = 91$ mM^{-1} cm^{-1} at 448 nm for the reduced CO-complex.

Product Analysis. Enzymatic oxidation of codeine was performed by mixing 30 μM P_{450} 2D6, 10 mM codeine, and 600 μM of cumene hydroperoxide (as electron donor) in 0.1 M phosphate buffer, pH 8.0. The reaction mixture (15 mL) was incubated in an open beaker for 3 h. The reaction was stopped by addition of 10 mL of 1 M NaOH. The solution was extracted with ethyl acetate (2×10 mL), and the combined organic extracts were washed with water and evaporated to dryness under a stream of nitrogen gas. The residue was redissolved in 5 mL of 0.1 M phosphate buffer, pH 6.0, containing 3% acetonitrile. One hundred microliters of this was analyzed by HPLC (Gilson) using a C_{18} reverse-phase column (S5 ODS2, 0.46×25 cm; Phase Separations Ltd., Clwyd, U.K.) eluted by a 40 mL gradient from 3% to 97% of acetonitrile in 0.1 M phosphate, pH 6.0, at 1 mL/min, with detection at 278 nm. Compounds eluting from the column were identified by ^{1}H NMR and electrospray mass spectrometry (Kratos Concept).

Optical Spectroscopy. UV−visible spectra were obtained essentially as described previously (Modi et al., 1995a). Equilibrium constants for substrate binding were estimated by fitting the following equation [see, e.g., He et al. (1991)] to the changes in absorbance at 418 nm:

$$\Delta A = \frac{\Delta A_\infty}{2E}[E + S + K_d - (\{E + S + K_d\}^2 - 4ES)^{1/2}] \quad (1)$$

where E and S represent the concentrations of P_{450} 2D6 and substrate, respectively, ΔA and ΔA_∞ are the changes in absorption at, respectively, the substrate concentration S and at saturating substrate concentration, and K_d is the equilibrium dissociation constant of the enzyme−substrate complex.

NMR Spectroscopy. Proton NMR measurements were predominantly carried out at 600 MHz, using a Bruker AMX600 spectrometer; studies of the frequency dependence of relaxation rates additionally involved measurements at 300 and 500 MHz. Experiments were carried out, and the data analyzed, essentially as described previously (Modi et al., 1995a). In particular, the longitudinal relaxation rate, $R_{1,obs}$, is given by

$$(R_{1,obs} - R_{1,d}) - R_{1,f} = \frac{E_0}{K_d + S_0}(R_{1,P} - R_{1,f}) \quad (2)$$

where E_o and S_o are the total enzyme and substrate concentrations, respectively, and K_d is the dissociation constant of the enzyme-substrate complex. $R_{1,P}$ is the paramagnetic contribution to the relaxation rate of the protons in the bound substrate due to the unpaired electrons of the heme iron, $R_{1,f}$ is the relaxation rate of the free substrate, and $R_{1,d}$ is the relaxation rate measured under the same conditions but with a diamagnetic control, in this case the reduced carbon monoxide complex of the enzyme. (The codeine proton relaxation rate in the presence of the reduced CO-complex was found to be identical to that in buffer, indicating that the diamagnetic contribution to relaxation was negligible.) By measuring ($R_{1,obs} - R_{1,d}$) as a function of protein and/or substrate concentration, estimates of K_d and $R_{1,P}$ can be obtained by fitting the data to eq 2.

The paramagnetic contribution, $R_{1,P}$, to the relaxation rate of the protons of bound substrate arising from the unpaired electrons on the heme iron, is related to the iron−proton distance by the Solomon−Bloembergen equation (Solomon

& Bloembergen, 1956; Dwek, 1973; Jardetzky & Roberts, 1981):

$$R_{1,P} = \frac{1}{T_{1,M}} = \frac{2}{15}\frac{\gamma_I^2 g^2 S(S+1)\beta^2}{r^6}\left(\frac{3\tau_c}{1+\omega_I^2\tau_c^2} + \frac{7\tau_c}{1+\omega_S^2\tau_c^2}\right) \quad (3)$$

where r is the distance of the proton from the heme iron, ω_I and ω_S are the nuclear and electronic Larmor frequencies, respectively, and τ_c is the effective correlation time of the dipolar interaction. The assumptions underlying the use of this equation are outlined in Jardetzky and Roberts (1981). The distances are calculated assuming location of the unpaired electrons on the iron; work on a range of heme proteins where NMR and crystallographic distances can be compared [e.g., for the coordinated water in cytochromes P_{450} *cam* and BM3; Philson et al., 1979; Modi et al., 1995a)] has shown that the delocalisation of the unpaired electrons into the porphyrin introduces no significant error into the distance estimates. The correlation time (τ_c) for P_{450} 2D6 was estimated by measuring $R_{1,P}$ at three frequencies (300, 500, and 600 MHz) and fitting the data to eq 3 [see, e.g., Modi et al. (1995a)].

Modeling of P_{450} 2D6. A set of models of the P_{450} 2D6−codeine complex was produced using homology modeling in conjunction with the distance restraints obtained from the paramagnetic relaxation effects. The sequence alignment used for homology modeling was based on the structural superposition of the three P_{450}s whose structures are currently available from the Brookhaven Protein Data Bank (PDB; Bernstein et al., 1977; Abola et al., 1987): P_{450} *cam* (PDB accession number 2CPP), P_{450} *terp* (1CPT), and P_{450} BM3 (2HPD). Initially, we aligned the sequence of P_{450} 2D6 against the structure-based multiple sequence alignment, containing 16 P_{450} sequences, of Hasemann et al. (1995) using the program Clustal V (Higgins et al., 1992). We subsequently refined this using Cameleon (Oxford Molecular Ltd.) to remove steric problems—particularly deviations from ideality of bond length and bond angle—that occurred consistently across our set of models. The alignment we used for modeling is shown in Figure 7; it differs only slightly—primarily in the exact positioning of gaps—from that reported by Hasemann et al. (1995).

Homology modeling was performed using the program Modeller (Sali & Blundell, 1993). Models were built containing only heavy atoms since the three crystal structures on which they are based do not contain hydrogen atoms, and the resulting models are likely to be only a first approximation to the three-dimensional structure of P_{450} 2D6. Modeller has the advantage over other homology modeling programs of allowing experimentally derived distance restraints to be used in conjunction with restraints from the homologous structures in deriving the model. Therefore, once we had added codeine to the Modeller library (with the aid of Quanta; Molecular Simulations Inc., Burlington, MA), we were able to produce a set of models which were generated with both the heme and the codeine present. The position of the codeine was defined partly by nonbonded intermolecular interactions between itself and both the protein and the heme and partly by the distance restraints derived from the NMR data. A total of 22 distance restraints, defining 11 upper and 11 lower bounds, were used; these were defined in terms of the carbon atom to which the respective proton was attached. Lower bounds were thus defined as the experimentally determined Fe···H distance minus 10% (a generous estimate of the experimental uncertainty) minus 1 Å (the C−H bond distance) and upper bounds as the experimentally determined distance plus 10% plus 1 Å. Additionally, because of the anticipated interaction between the basic nitrogen in codeine and the carboxyl group of Asp 301 (see below), the distance between this nitrogen and OD1 of Asp 301 was given an upper bound restraint of 4.5 Å. A total of 45 models were produced and refined within Modeller. Conformational clustering of the final models, and identification of structures "representative" of the ensemble of models, was performed using the program NMRCLUST (Kelley et al., 1996).

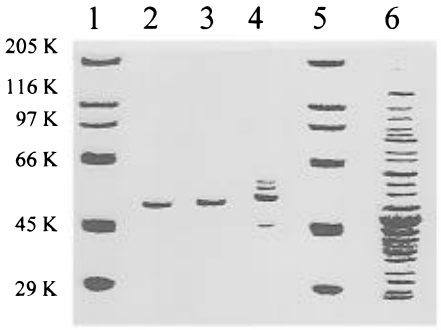

FIGURE 2: SDS−polyacrylamide gel (8%) electrophoresis of the protein samples following each purification step. (Lanes 1 and 5) Molecular weight markers; (lane 6) Cell lysate after homogenisation; (lane 4) After first nickel column; (lane 3) After proteolysis with thrombin and second nickel column; and (lane 2) After monoQ FPLC column. Samples with the oligohistidine sequence attached (lane 4) run at slightly higher molecular mass than after the removal of this sequence by thrombin (lanes 2 and 3), when the protein runs close to its expected molecular mass of 50 kDa.

RESULTS AND DISCUSSION

Expression and Purification of P_{450} 2D6. The availability of pure, active P_{450} 2D6 in the quantities required for structural studies has hitherto been limited. In a recent report of an *Escherichia coli* expression system for P_{450} 2D6 (Gillam et al., 1995), the expressed detergent-solubilized protein had incorporated only about 50% of the expected heme. In addition, the reduced-CO complex retained a significant absorbance at 420 nm, suggesting that the protein which had incorporated heme was not fully native. We therefore decided to use a baculovirus expression system. We have earlier reported expression of unmodified P_{450} 2D6 in baculovirus (Paine et al., 1996) and have now adapted this system to enable the affinity purification of the expressed P_{450} 2D6 through the addition of an oligohistidine sequence, together with a thrombin cleavage site to allow for removal of this sequence after purification, at the C-terminus of the enzyme. Using this construct in the baculovirus/Sf9 cell system, we obtained expression of P_{450} 2D6 at the level of 5% of the total cell protein, and the presence of the oligohistidine sequence facilitated purification to >90% homogeneity in 36% yield. The progress of the purification is summarized in Table 1, and Figure 2 shows the SDS−polyacrylamide gel electrophoresis analysis at each step.

The purified recombinant P_{450} 2D6 shows optical spectra typical of a cytochrome P_{450}, that is, in the oxidized state a spectrum with well resolved α and β bands at 570 and 535 nm and a strong Soret band at 418 nm, while the spectrum

Table 1: Purification of Recombinant P450 2D6

purification step	total protein (mg)	P_{450} content (nmol/mg)	recovery of P_{450} 2D6 (%)	purity[a]
cell lysate	123	0.99	(100)	5.0
eluate from first nickel column	3.4	17.0	47.5	85.0
after thrombin cleavage and passage through nickel column	2.8	17.1	39.3	85.5
eluate from Mono Q column	2.4	18.3	36.1	91.5

[a] Based on the theoretical P450 content of 20.0 nmole/mg protein.

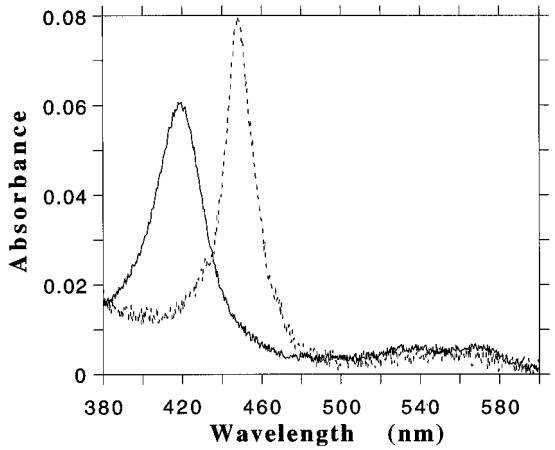

FIGURE 3: Visible absorption spectra of 0.87 μM recombinant P_{450} 2D6 (—), and of its reduced CO complex (- - -) in 0.1 M phosphate buffer (pH 8.0).

of the CO-complex of the reduced enzyme shows peaks at 547 and 448 nm (Figure 3). The absence of any band at 420 nm in the CO-complex of the reduced enzyme shows that there is no inactive P_{450} in the preparation (Modi et al., 1995b). The heme content of the purified recombinant P_{450} 2D6, determined from the spectrum of the CO-complex of the reduced enzyme, was determined to be 18.3 nmol/mg (Table 1); this corresponds to >90% incorporation of heme. The baculovirus/Sf9 cell expression system is clearly able to incorporate heme into the P_{450} 2D6 polypeptide efficiently. The overall yield of protein from 700 mL of insect cell culture was 2.4 mg, sufficient for structural analysis.

Interaction of Codeine and Bufuralol with P_{450} 2D6. On addition of increasing concentrations of the substrates codeine or bufuralol to P_{450} 2D6, the intensity of the Soret band of the oxidized enzyme at 418 nm decreased, while the intensity of bands at 390 and 650 nm increased (data not shown). The band at 650 nm is characteristic of high spin ferric heme proteins (Falk, 1964). Similar spectral changes on the formation of the complex of substrate with the Fe(III) form of the enzyme have been observed in other cytochromes P_{450} and have been attributed to a change in spin state of the heme iron from low spin ($S = 1/2$) to high spin ($S = 5/2$) (Dawson, 1988; Sariaslani, 1991). The crystal structures of cytochrome P_{450}s show that a water molecule (or a hydroxide ion) is present in the sixth coordination position of the heme iron in the absence of substrate [e.g., Poulos et al. (1986) and Ravichandran et al. (1993)] and is expelled on binding of the substrate [e.g., Poulos et al., 1987; Modi et al., 1995a]. The presence of a strong-field (aquo) ligand axially coordinated to the iron atom leads to maximal pairing of the 5d electrons of the iron to give a net spin of 1/2, whereas on substrate binding the absence of such a strong-field ligand leads to maximal unpairing of the d electrons to give a net spin of 5/2.

The dependence of these changes on the concentration of substrates (Figure 4) can be used to estimate the equilibrium

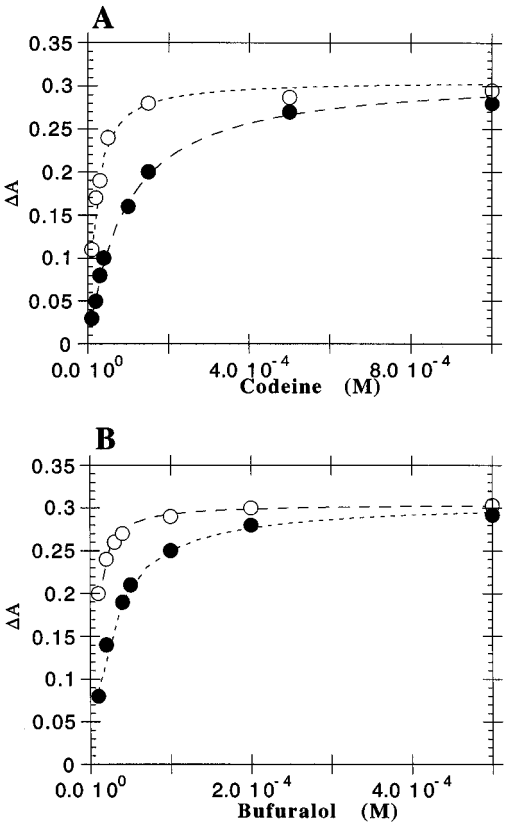

FIGURE 4: Changes in absorbance at 418 nm for P_{450} 2D6 (5.2 μM) in 0.1 M phosphate buffer (pH 8.0) (open symbols) and in phosphate buffer plus 0.2 M KCl (filled symbols) as a function of codeine (A) and bufuralol (B) concentration. The dotted lines are the least-squares fit of eq 1 to the data.

Table 2: Substrate Binding to Recombinant P_{450} 2D6

substrate	method[a]	[KCl] (mM)	[pyridine] (mM)	K_d (μM)	ΔA_∞
codeine	optical	0	0	15 (± 1)	0.307 (± 0.004)
	optical	200	0	87 (± 4)	0.313 (± 0.003)
	NMR	200	0	115 (± 23)	
	NMR	200	0.3	615 (± 87)	
bufuralol	optical	0	0	3.9 (± 0.3)	0.305 (± 0.002)
	optical	200	0	22.3 (± 0.6)	0.308 (± 0.002)

[a] Optical, from absorbance changes at 418 nm; NMR, from paramagnetic relaxation effects on substrate protons. All experiments were carried out at 27 °C in 0.1 M phosphate buffer, pH 8.0.

constant for substrate binding, by using eq 1; the results obtained with codeine and bufuralol are summarized in Table 2. The value of ΔA_∞ is in each case consistent with a complete spin-state conversion at saturating substrate concentrations. Addition of 0.2 M KCl causes a significant decrease in the affinity of the substrate for the enzyme, suggesting an electrostatic component to the interaction (see below).

The fate of codeine on oxidation by the purified P_{450} 2D6 (using cumene hydroperoxide as electron donor; Penman et

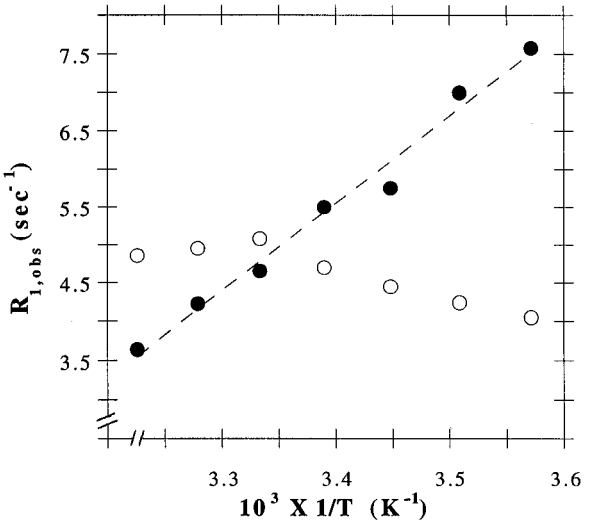

FIGURE 5: Temperature dependence of the spin−lattice relaxation rate of the methoxy proton NMR resonance of codeine. Measurements were made at 600 MHz with 30 mM substrate and 1 μM P_{450} 2D6 in 0.1 M phosphate buffer, pH 8.0, in the absence (open circles) and presence (filled circles) of 0.2 M KCl.

al., 1993) was determined by HPLC separation of the metabolites on a C_{18} reverse-phase column and identification by ^{1}H NMR and mass spectrometry. A single product was observed eluting earlier in the gradient (11.3 min) than the codeine substrate (14.7 min), which was identified as morphine, the product of O-demethylation of codeine. The time course of the oxidation of codeine to morphine by P_{450} 2D6 was measured by monitoring the build-up of the HPLC peak area of the product over a period of 30 min, leading to an estimate for the catalytic rate (k_{cat}) of 7.7 min^{-1}. Codeine oxidation has not previously been directly measured with purified P_{450} 2D6; although P_{450} 2D6 can catalyze some N-demethylation reactions (Coutts et al., 1994), it is clear from studies of CYP2D6 polymorphism in human populations that, *in vivo*, P_{450} 2D6 catalyzes only O-demethylation and not N-demethylation of codeine (Mortimer et al., 1990; Desmeules & Dayer, 1991; Ladona et al., 1991). Rates of 1.04 min^{-1} for debrisoquine 4-hydroxylation and 1.23 min^{-1} for (±)bufuralol 1′-hydroxylation have been reported for recombinant P_{450} 2D6 expressed in *E. coli*, using NADPH-cytochrome P_{450} reductase as the electron donor (Gillam et al., 1995).

Structural Studies of Codeine Binding. Measurements of the paramagnetic relaxation effects of the heme iron on the protons of the substrate can be used to obtain estimates of distances between individual protons of the bound substrate and the heme iron of P_{450} 2D6, as described previously for P_{450} BM3 (Modi et al., 1995a). Use of this method requires (i) demonstration that the substrate is exchanging rapidly (relative to the spin−lattice relaxation rate) between the bound and free states, and (ii) determination of a value for τ_c, the correlation time of the dipolar interaction between the nuclear and electron spins.

In order to establish whether exchange was fast on the relaxation time scale, the temperature dependence of the spin−lattice relaxation rate ($R_{1,obs}$) of codeine protons in the presence of the enzyme was measured in 0.1 M phosphate buffer, pH 8.0, with and without 0.2 M KCl (Figure 5). In the absence of added salt, the observed behavior is characteristic of intermediate exchange, relaxation being exchange-limited at low temperatures and only approaching fast

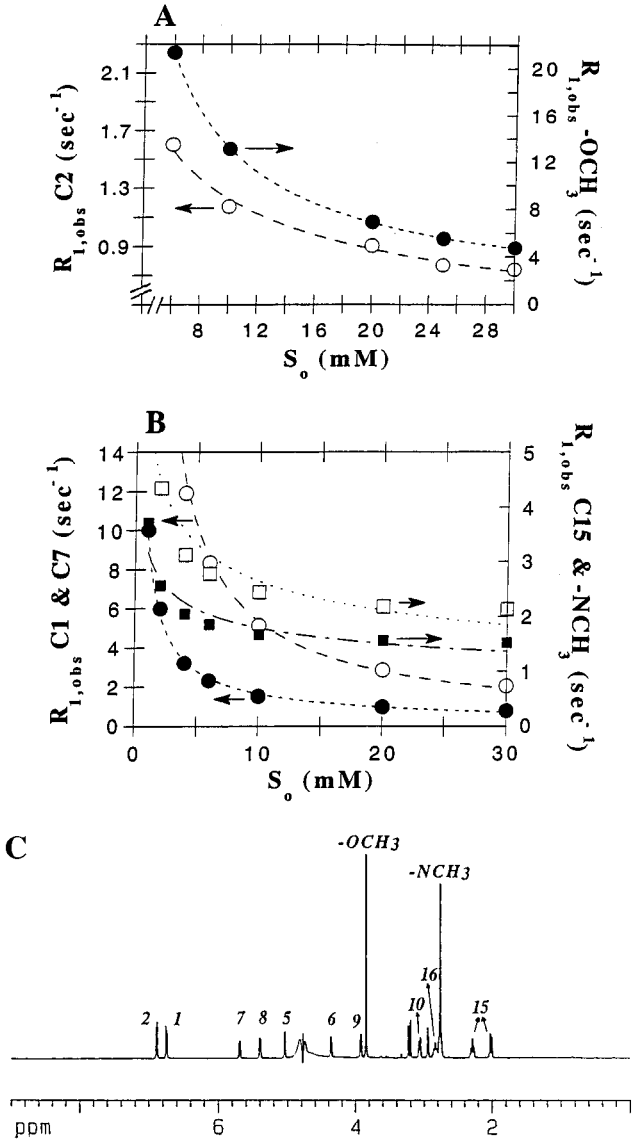

FIGURE 6: Measured spin−lattice relaxation rates for protons of codeine as a function of codeine concentration in the presence of P_{450} 2D6. (A) With 1 μM P_{450} 2D6; filled circles represent data for -OCH_3 and open circles that for C2 protons, respectively. (B) With 70 μM P_{450} 2D6. Filled circles and squares represent data for C7 and -NCH_3, respectively; open circles and squares represent data for C1 and C15, respectively. Lines represent the least-squares fit of eq 2 to the experimental data. (C) Proton spectrum of codeine showing the resonance assignments.

exchange at the highest temperature used (310 K). However, in the presence of the added salt, where codeine binding is 6-fold weaker (Table 2), a linear increase in $R_{1,obs}$ as a function of reciprocal temperature was observed across the range 283−310 K, demonstrating that the fast exchange condition is satisfied in this case. Figure 6 shows only the temperature dependence of the methoxy resonance of codeine, for which the paramagnetic relaxation effects are greatest, but a closely similar temperature dependence was observed for each of the other resonances of codeine. Therefore, all subsequent NMR relaxation experiments were carried out in 0.1 M phosphate buffer, 0.2 M KCl, pH 8.0. Similar experiments with bufuralol, which binds ~4-fold more tightly than codeine (Table 2), showed that even in the presence of 0.2 M KCl the fast exchange condition was not fully satisfied (data not shown), and the relaxation experiments with this substrate were not pursued further. Measurement of the frequency dependence of the relaxation

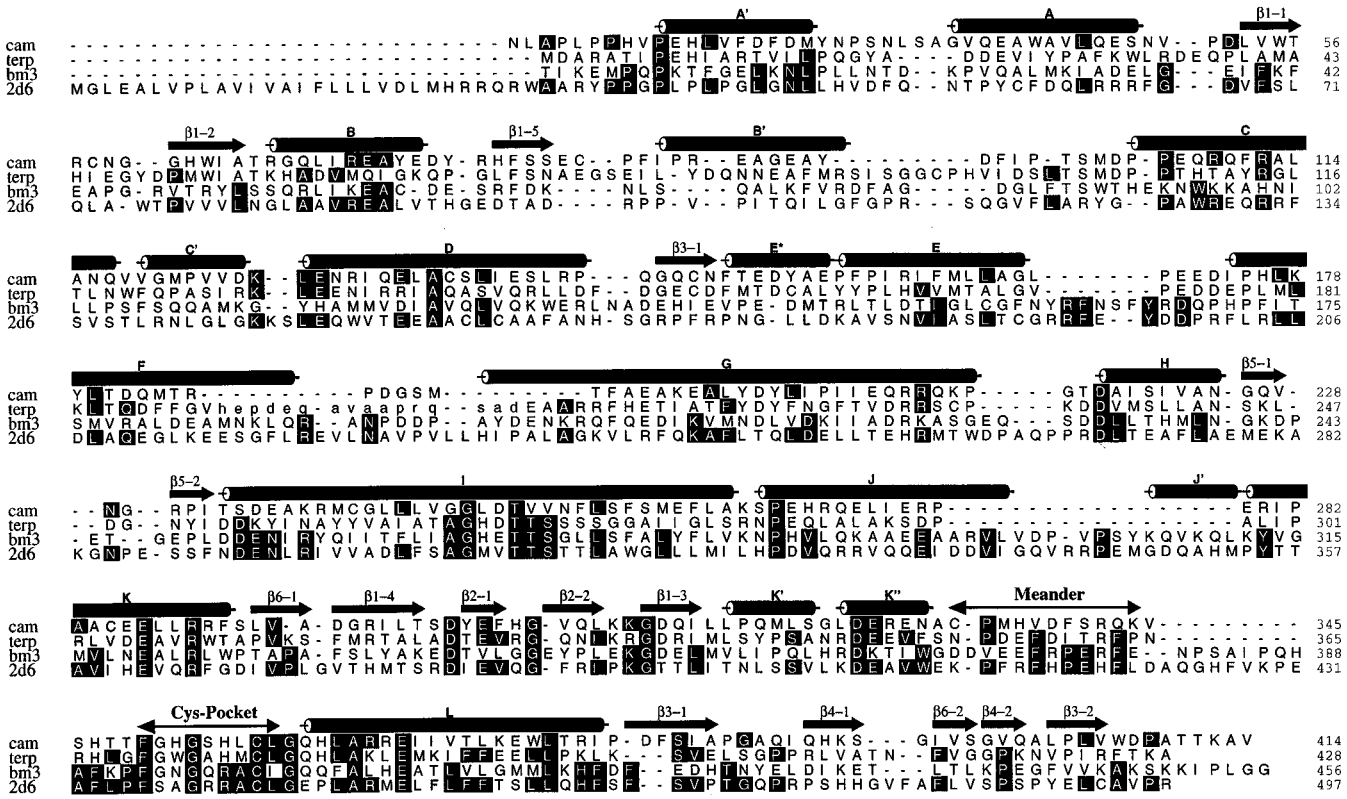

FIGURE 7: Multiple sequence alignment used for modeling. Those residues in the other three P_{450}s which are identical to P_{450} 2D6 are shown on a black background. The extent of the secondary structure shown at the top of the alignment is taken from Hasemann et al. (1995). Note that (i) residues 191−207 of P_{450} *terp* are missing from the crystal structure and are shown in lowercase, and (ii) a further 13 P_{450} sequences were used in obtaining this alignment.

rates of the codeine protons [see Materials and Methods and Modi et al. (1995a)] allowed the determination of the correlation time τ_c. The value obtained, 3.3×10^{-10} s, is comparable to the values reported for other cytochromes P_{450} (Griffin & Peterson, 1975; Philson et al., 1979; Woldman et al., 1985; Jacobs et al., 1987; Crull et al., 1989; Castro-Maderal & Sullivan, 1992; Modi et al., 1995a) whose average is 3×10^{-10} s; for these enzymes, τ_c is determined by the electron spin-lattice relaxation time, τ_s, and it appears that a large τ_s value is a characteristic of cytochromes P_{450}.

Spin−lattice relaxation rates were measured at different codeine concentrations, with the concentration of the P_{450} 2D6 held constant in a given experiment; because the relaxation effects of the heme iron on different substrate protons differ by several orders of magnitude, a series of experiments were carried out at different protein concentrations (1−70 μM) to permit precise measurements for all the resolved proton resonances. Data for six well-resolved resonances of codeine, together with the spectrum of codeine, are shown in Figure 6. After each set of experiments, optical spectra of the reduced CO-complex were measured to ensure that P_{450} had not been converted into inactive P_{420} during the course of the experiments. The average value for K_d obtained by fitting eq 2 to the data in Figure 6 (115 ± 23 μM) is in satisfactory agreement with that obtained from optical spectroscopy (Table 2); use of a version of eq 2 in which the stoichiometry is a variable gave an estimate of 1.0 (± 0.2) molecules of substrate bound per molecule of P_{450} 2D6. These results confirm that exchange is rapid and that the optical and NMR spectroscopy experiments are each reporting on the binding of the same substrate molecule.

The spin−lattice relaxation times of the bound substrate, $T_{1,M}$, and the estimated iron−proton distances for codeine bound to P_{450} 2D6 are summarized in Table 3. These measurements give a very clear indication of the orientation of the codeine molecule in the active site of the enzyme, the protons of the methoxy group being only 3.10 Å away from the heme iron, while those of the N-methyl group are 12.1 Å away. The observation that when codeine is bound to the enzyme, the methoxy group is very much closer to the

Table 3: Paramagnetic Relaxation Times and Distances from Protons of the Bound Codeine to the Heme Iron of P_{450} 2D6[a]

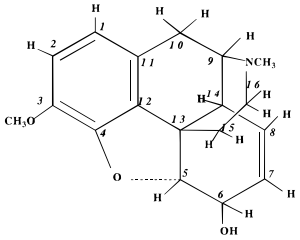

	proton	$T_{1,M}$ (ms)	r (Å)
codeine	C1H	1.6 (± 0.3)	7.5 (± 0.2)
	C2H	0.14 (± 0.01)	5.0 (± 0.1)
	-OCH_3	0.0078 (± 0.0009)	3.1 (± 0.1)
	C5H	5.1 (± 0.4)	9.1 (± 0.1)
	C6H	9.0 (± 0.7)	10.0 (± 0.2)
	C7H	5.6 (± 0.9)	9.3 (± 0.3)
	C8H	10.0 (± 0.8)	10.2 (± 0.2)
	C9H	17.7 (± 1.2)	11.2 (± 0.2)
	$C10H_2$	7.8 (± 0.4)	9.8 (± 0.1)
	$C15H_A$	5.7 (± 0.3)	9.3 (± 0.1)
	$C15H_B$	14.2 (± 0.9)	10.8 (± 0.2)
	-NCH_3	28.0 (± 1.5)	12.1 (± 0.2)
codeine + 0.3 mM pyridine	-OCH_3	0.12 (± 0.05)	4.9 (± 0.3)
	C2H	1.0 (± 0.3)	7.0 (± 0.3)

[a] The resonances of the C14 and C16 protons were insufficiently resolved for accurate T_1 measurements.

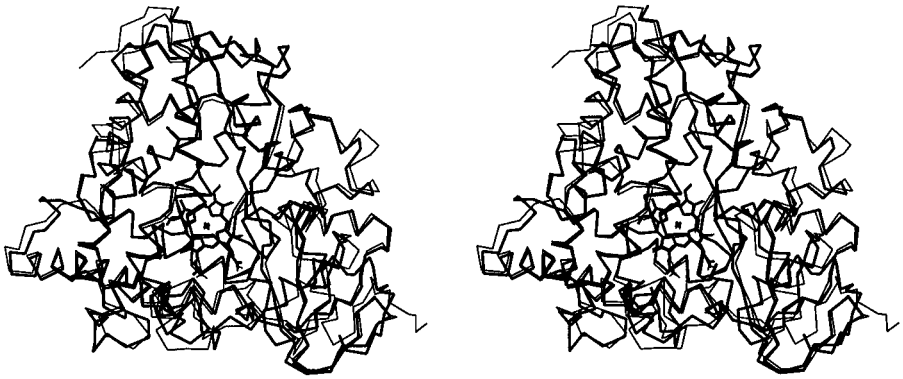

FIGURE 8: Stereoview of the overall fold of the "most representative" (Kelley et al., 1996) model of P450 2D6 (thick lines) compared with the structure of P450 BM3 (thin lines; Ravichandran et al., 1993).

iron than is the N-methyl group clearly indicates that the enzyme will catalyze O-demethylation of codeine and not N-demethylation. This is in accord with *in vivo* observations and with our measurements on the purified enzyme (see above).

In this P_{450}−substrate complex, the substrate is bound close to the heme, the nearest protons being only 3.1 Å away. The crystal structure of the camphor complex of P_{450} *cam* also shows the substrate bound in close proximity to the heme (Poulos et al., 1987), whereas in the laurate complex of the heme domain of cytochrome P_{450} BM3 the substrate approaches no nearer than 7 Å to the heme iron (Modi et al., 1995a). This comparison was extended by studying the binding of codeine in the presence of 0.3 mM pyridine. Pyridine has been shown to bind very tightly to the heme iron of cytochromes P_{450} (Griffin & Peterson, 1972; Banci et al., 1994). In the presence of pyridine, there was no change in the optical spectrum of P_{450} 2D6 on addition of a >100-fold excess of codeine (data not shown); in the presence of pyridine, the heme iron does not undergo the spin state conversion on addition of even a large excess of codeine, since the substrate is unable to expel the strongly bound pyridine. The paramagnetic relaxation experiments show that codeine binds 7-fold more weakly in the presence of 0.3 mM pyridine (Table 2) but also binds in a different position in the active site, farther away from the heme iron (Table 3). This is consistent with the model of the enzyme−substrate complex described below (Figure 8), where there is not sufficient space between the methoxy group of codeine and the heme to accommodate a pyridine molecule. It has recently been shown that pyridine and camphor cannot bind simultaneously to P_{450} *cam* (Banci et al., 1994); the formation of a ternary complex with camphor has been suggested only for small molecules such as cyanide (Shiro et al., 1989). For P_{450} BM3, on the other hand, the substrate laurate binds in the same position and with very similar affinity in the presence and absence of pyridine (Modi et al., 1995a).

Structural Models of Cytochrome P_{450} 2D6. Models of the complex of codeine with P_{450} 2D6 were generated, as described in Materials and Methods, by a combination of homology modeling, using the available crystal structures and the sequence alignment shown in Figure 7, with the distance constraints derived from the relaxation experiments. Many models of the active site of P_{450} 2D6 have postulated the involvement of a carboxylate group forming an interaction with the basic nitrogen of the substrate molecules (Wolff et al. 1985; Meyer et al., 1986; Islam et al., 1991; Koymans et al., 1992), and this has been proposed to be aspartate 301 (Islam et al., 1991). Examination of our initial models showed that the positively charged nitrogen atom of codeine is indeed positioned close to Asp301, and the results of recent mutagenesis experiments (Ellis et al., 1996) in which Asp301 has been replaced by Glu, Gly or Asn provide further evidence for the involvement of this residue in substrate binding. We therefore added an additional constraint in the model-building process, setting an upper bound restraint of 4.5 Å to the distance between the nitrogen of codeine and OD1 of Asp 301.

Table 4: RMS Deviations between the Models of P_{450} 2D6 and the Three Available Crystal Structures

crystal structure	RMS deviation (Å)[a]
P_{450} *cam* (Poulos et al., 1985)	1.9 ± 0.1
P_{450} *terp* (Hasemann et al., 1994)	1.7 ± 0.1
P_{450} BM3 (Ravichandran et al., 1993)	1.0 ± 0.1

[a] Calculated for C_α atoms of topologically equivalent residues across the final 13 models of P_{450} 2D6.

In this way, a total of 45 models of the P_{450} 2D6−codeine complex were generated. These provide the first model for the active site of a mammalian cytochrome P_{450} based on direct structural constraints. They were evaluated on the basis of their bonded and nonbonded interactions and their violations of the NMR-derived distance restraints. Thirty-two of the models were discarded, leaving 13 models which were taken to be acceptable representations of the three-dimensional structure of the complex and on which the following discussion is based.[2]

The overall fold of a representative member of this set of models is shown in Figure 8, where it is compared with that of P_{450} BM3; as shown in Table 4, our models are more similar to P_{450} BM3 than to P_{450} *terp* or P_{450} *cam*. This agrees with the prediction of Hasemann et al. (1995) that the eukaryotic enzymes will adopt this topology, and with the suggestion (Lewis, 1995) that P_{450} 2D6 is more similar to P_{450} BM3 than to either P_{450} *cam* or P_{450} *terp*. The RMS deviations across the ensemble of 13 models, determined using residues from Arg 28 to the C-terminus, are 1.4 (±0.3) Å for the backbone atoms, and 2.2 (±0.2) Å for all the non-hydrogen atoms. (We have little confidence in modeling residues 1−27 because of the absence of structural information for these residues.) RMS deviations of the backbone atoms of each residue from the unminimized average structure are shown in Figure 9. The largest deviations occur

[2] Coordinates of these models are available on e-mail request to gcr@le.ac.uk.

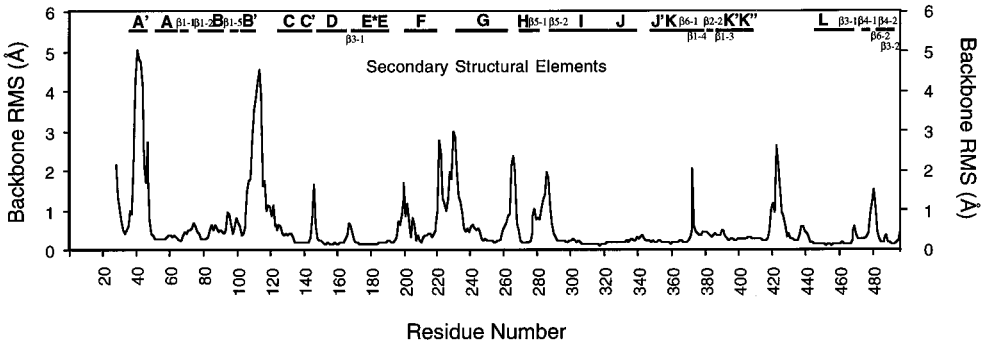

FIGURE 9: Backbone RMS values from the unminimised average structure for the final set of 13 models of P_{450} 2D6.

in the A′ helix, at the C-terminal end of helix B′, in the F−G loop, and in the G−H and H−I loops, regions which vary considerably between the three available crystal structures (Hasemann et al., 1995). On the other hand, as would be expected, regions of the structure such as the I, J, and K helices which are closely similar in the three crystal structures are well-defined in our models. It is notable that the relative orientation of the F and G helices is similar to the corresponding region in P_{450} BM3 and P_{450} *terp* but differs from that in P_{450} *cam*, in which the F−G loop is much shorter; as Hasemann et al. (1995) point out, eukaryotic P_{450}s, including P_{450} 2D6, are in general characterized by longer F−G loops and thus would be expected to have the topology seen for P_{450} BM3 and P_{450} *terp*.

The region of the structure involved in binding the heme, including the "Cys-pocket", is in general well-defined in the models. In the structures of other P_{450}s, there are conserved interactions with the heme propionates (Hasemann et al., 1995). Two residues in helix C, H110 and R114 in P_{450} *terp*, interact with the D-ring propionate; in P_{450} 2D6 the corresponding residues are W128 and R132, and the interaction with the propionate is conserved in all 13 of our models. In P_{450} *cam* and P_{450} *terp*, the A-ring propionate forms an ion pair with an arginine on β1−4 equivalent to H376 in P_{450} 2D6, while in P_{450} BM3 this role is performed by K69 in β1−5. In our P_{450} 2D6 models, H376 could fulfill this role in all 13 models, while R101 (only one residue away from K69 of P_{450} BM3 in our alignment) is appropriately placed in four of the 13 models. Hasemann et al. (1995) noted that the "meander" part of the structure is stabilized by interactions involving an arginine and a glutamate in the K helix and a second arginine in the meander region. In our alignment of P_{450} 2D6, the corresponding residues are E362, R365, and H419, and in nine of the models His 419 forms a hydrogen bond with the main chain carbonyl group of E410, equivalent to an interaction formed by the corresponding arginine residue in the other P_{450}s.

It has been proposed that the catalytic mechanism of P_{450}s involves the delivery of a proton to the iron-bound oxygen by the conserved threonine in helix I (T309 in P_{450} 2D6), aided by the neighboring conserved acidic residue [e.g., Raag et al. (1991) and Gerber and Sligar (1992)]. It is noteworthy that this conserved acidic residue is absent from P_{450} 2D6, in which the corresponding residue is Val 308, and from some other eukaryotic P_{450}s. We have been unable to identify an alternative proton source in our model of P_{450} 2D6; Hasemann et al. (1995) suggest that, at least in P_{450} *terp* and P_{450} BM3, the requisite proton may be transferred by bound water molecules.

The codeine binding site is predominantly hydrophobic in nature, the contact residues comprising Pro 103 (in 10 out of the 13 models), Ile 106 (13/13), Thr 107 (11/13), Leu 110 (9/13), Pro 114 (8/13), Ala 122 (13/13), Asp 301 (13/13), Ser 304 (13/13), Ala 305 (13/13), Thr 309 (12/13), Val 370 (13/13), Phe 483 (13/13), and the heme (Figure 10a,b). The involvement of Phe 483, toward the C-terminus of the molecule, is particularly interesting, as this residue has not previously been associated with substrate binding to P_{450} 2D6. The methoxy oxygen of the most representative codeine is 4.5 Å from the heme iron (range 3.8−5.7 Å across the set of 13 models) and is almost directly above the A ring of the heme. This differs from the model of Islam et al. (1991), in which this oxygen is positioned almost directly above the iron. The carbon−oxygen bond in the codeine methoxy group is appropriately oriented for reaction with the iron-bound oxygen (Figure 10c). In our models the distance between the heme iron and the basic nitrogen of the codeine is 10.5 Å (9.6−11.3 Å), somewhat shorter than the distance of 11.5 Å in the Islam et al. (1991) model; our models indicate that the position defined by Islam et al. (1991) for the codeine would lead to steric clashes with residues in the I helix and with Pro 114. In eight of the models there is a possible hydrogen bond between the hydroxyl group of the codeine and the carbonyl oxygen of Gly 373. There is also a possible hydrogen bond between this hydroxyl group and the A-ring propionate of the heme in seven of the models. We have recently shown by heme replacement experiments in cytochrome P_{450} BM3 that the carboxylate of this propionate group can influence substrate binding (Modi et al., 1995b). The two possible configurations about the basic nitrogen on the codeine are both observed across the 13 models—three in the same configuration as in the crystal structure of codeine and ten in the other, thereby orientating the hydrogen on the basic nitrogen toward the carboxyl group of Asp 301 in 10 of the 13 models. Asp 100, previously proposed as a candidate for interaction with this basic nitrogen (Koymans et al., 1993), is situated away from the binding site, roughly in the plane of the heme beyond the two propionate groups. The identification of Asp 301 rather than Asp 100 as the anionic residue involved in substrate binding is in agreement with our recent mutagenesis work (G. Smith and C.R.W., unpublished work). The side chain of Asp 301 adopts essentially two different orientations across the 13 models, either "vertical" (χ_1 *gauche*$^+$; 8/13 models) or "horizontal" (χ_1 *trans*; 5/13 models) in the orientation of Figure 10a. Substrates for P_{450} 2D6 fall into two classes, in which there is a separation of either 5 or 7 Å between the basic site and the site of reaction (Koymans et

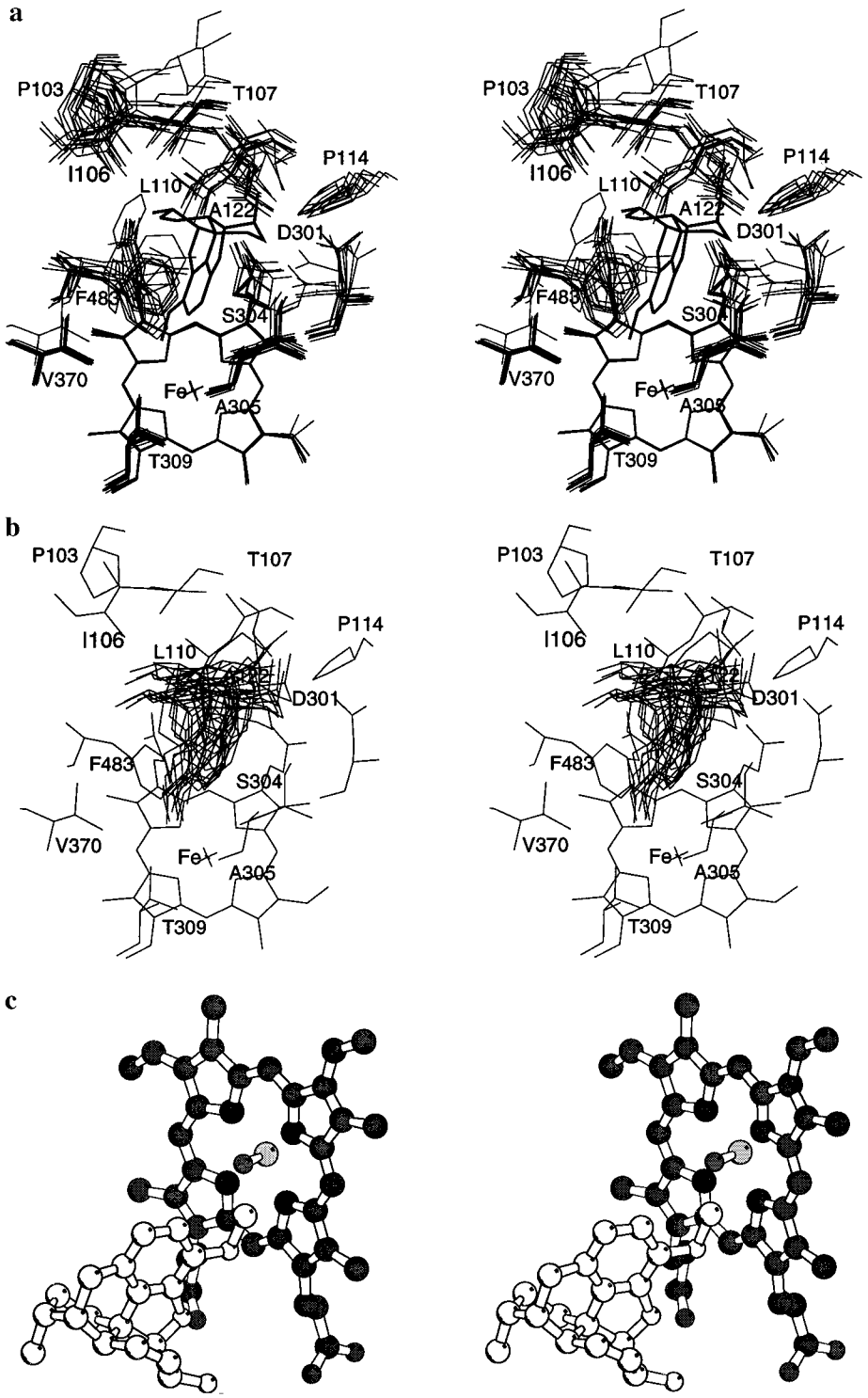

FIGURE 10: Stereoviews of the codeine binding site of P_{450} 2D6 following superposition of the heme moieties of the models. (a) A single codeine molecule (the "most representative" codeine orientation; Kelley et al., 1996), is shown in thick lines, and the residues defining the codeine binding site are shown for all the 13 final models. (b) The same view as panel a, with the 13 codeine molecules and the residues defining the codeine binding site in the "most representative" protein. (c) Ball and stick representation showing the position of the "most representative" codeine, and particularly the methoxy carbon−oxygen bond, with respect to the heme. The oxygen atom bonded to the heme iron has also been modeled in.

al., 1992). In the "horizontal" (χ_1 *trans*) side chain orientation, Asp 301 would be positioned in such a way that its carboxylate would be able to interact with the basic site on both classes of substrate [see Koymans et al. (1992)]. Alternatively, this side chain could readily adopt a different orientation in the complexes of the enzyme with the two kinds of substrate.

In conclusion, we have shown that a compelling model of a cytochrome P_{450}−substrate complex can be generated from a combination of multiple structure and sequence alignment and direct experimental constraints derived from paramagnetic relaxation measurements. This model is consistent with the proposal that Asp 301 forms an ion pair with the basic nitrogen of codeine and identifies a number of other residues as forming the binding site for this substrate. Studies of mutants of P_{450} 2D6 designed on the basis of this initial model, as well as of other substrates, are in progress to refine the model and to use it as the basis for understanding

the specificity of the enzyme, and we are also using this approach in the study of other cytochromes P_{450}.

ACKNOWLEDGMENT

We are grateful to Mike Sternberg for supplying his coordinates for the P450 2D6 template and to Andrej Sali for his gift of the program MODELLER.

REFERENCES

Abola, E. E., Bernstein, F. C., Bryant, S. H., Koetzle, T. F., & Weng, J. (1987) in *Crystallographic Databases—Information Content, Software Systems, Scientific Applications* (Allen, F. H., Bergerhoff, G., & Sievers, R., Eds.) pp 107−132, Data Commission of the International Union of Crystallography, Bonn/Cambridge/Chester.

Arnold, F. H. (1991) *Bio/Technology 9*, 151−156.

Banci, L., Bertini, I., Marconi, S., Pierattelli, R., & Sligar, S. G. (1994) *J. Am. Chem. Soc. 116*, 4866−4873.

Bernstein, F. C., Koetzle, T. F., Williams, G. J. B., Meyer, E. F., Brice, M. D., Rodgers, J. R., Kennard, O., Shimanovichi, T., & Tasumi, M. (1977) *J. Mol. Biol. 112*, 535−542.

Bradford, M. M. (1976) *Anal. Biochem. 72*, 248−254.

Castro-Maderal, L., & Sullivan, P. D. (1992) *FEBS Lett. 296*, 249−253.

Coutts, R. T., Su, P., & Baker, G. B. (1994) *J. Pharmacol. Toxicol. Methods 31*, 177−186.

Crull, G. B., Kennington, J. W., Graber, A. R., Ellis, P. D., & Dawson, J. H. (1989) *J. Biol. Chem. 264*, 2649−2655.

Cupp-Vickery, J. R., & Poulos, T. L. (1995) *Nature Struct. Biol. 2*, 144−153.

Daly, A. K., Leathart, J. B. S., London, S. J., & Idle, J. R. (1995) *Human Genet. 95*, 337−341.

Dawson, J. H. (1988) *Science 248*, 433−439.

Desmeules, J., & Dayer, P. (1991) *Douleur Analgesie 4*, 79−86.

Dwek, R. A. (1973) *NMR in Biochemistry*, pp 11−142, Oxford University Press, London.

Eichelbaum, M., & Gross, A. S. (1990) *Pharmacol. Ther. 46*, 377−394.

Ellis, S. W., Ching, M. S., Watson, P. F., Henderson, C. J., Simula, A. P., Lennard, M. S., Tucker, G. T., & Woods, H. F. (1992) *Biochem. Pharmacol. 44*, 617−620.

Ellis, S. W., Smith, G., Wolf, C. R., Tucker, G. T., & Woods, H. F. (1995) *J. Biol. Chem. 270*, 29055−29058.

Falk, J. E. (1964) in *Porphyrins and Metalloporphyrins*, pp 131−190, Elsevier, New York.

Ferenczy, G. G., & Morris, G. M. (1989) *J. Mol. Graphics 7*, 206−213.

Gerber, N. C., & Sligar, S. G. (1992) *J. Am. Chem. Soc. 114*, 8742−8743.

Gillam, E. M. J., Guo, Z., Martin, M. V., Jenkins, C. M., & Guengerich, F. P. (1995) *Arch. Biochem. Biophys. 319*, 540−550.

Gonzalez, F. J., Skoda, R. C., Kimura, S., Umeno, M., Zanger, U., Nebert, D. W., Gelboin, H. V., Hardwick, J. P., & Meyer, U. A. (1988) *Nature 331*, 442−446.

Gough, A. C., Miles, J. S., Spurr, N. K., Moss, J. E., Gaedigk, A., Eichelbaum, M., & Wolf, C. R. (1990) *Nature 347*, 773−776.

Griffin, B. W., & Peterson, J. A. (1972) *Biochemistry 11*, 4740−4745.

Griffin, B. W., & Peterson, J. A. (1975) *J. Biol. Chem. 250*, 6445−6451.

Hasemann, C. A., Ravichandran, K. G., Peterson, J. A., & Deisenhofer, J. (1994) *J. Mol. Biol. 236*, 1169−1185.

Hasemann, C. A., Kurumbail, R. G., Boddupalli, S. S., Peterson, J. A., & Deisenhofer, J. (1995) *Structure 3*, 41−62.

He, S., Modi, S., Bendall, D. S., & Gray, J. C. (1991) *EMBO J. 10*, 4011−4016.

Higgins, D. G., Bleasby, A. J., & Fuchs, R. (1992) *CABIOS 8*, 189−191.

Islam, S. A., Wolf, C. R., Lennard, M. S., & Sternberg, M. J. E. (1991) *Carcinogenesis 12*, 2211−2219.

Jacobs, R. E., Singh, J., & Vickery, L. E. (1987) *Biochemistry 26*, 4541−4545.

Jardetzky, O., & Roberts, G. C. K. (1981) *NMR in Molecular Biology*, Academic Press, New York.

Kelley, L. A., Gardner, S. P., & Sutcliffe, M. J. (1996) *Protein Eng.* (submitted).

Kimura, S., Umeno, M., Skoda, R. C., Meyer, U. A., & Gonzalez, F. J. (1989) *Am. J. Hum. Genet. 45*, 889−904.

Koymans, L., Vermeulen, N. P. E., van Acker, S. A. B. E., te Koppele, J. M., Heykants, J. J. P., Lavrijsen, K., Meuldermans, W., & Donne-Op den Kelder, G. M. (1992) *Chem. Res. Toxicol. 5*, 211−219.

Koymans, L., Vermeulen, N. P. E., Baarslag, A., & Donne-Op den Kelder, G. (1993) *J. Comput.-Aided Mol. Des. 7*, 281−289.

Ladona, M. G., Lindstrom, B., Thyr, C., Dun-Ren, P., & Rane, A. (1991) *Br. J. Clin. Pharmacol. 32*, 295−302.

Lennard, M. S. (1990) *Pharmacol. Toxicol. 67*, 273−283.

Lewis, D. F. V. (1995) *Xenobiotica 25*, 333−366.

Loida, P. J., & Sligar, S. G. (1993) *Biochemistry 43*, 11530−11538.

Meyer, U. A., Gut, J., Kronbach, T., Skoda, C., Meier, U. T., & Catin, T. (1986) *Xenobiotica 16*, 449−464.

Meyer, U. A., Skoda, R. C., & Zanger, U. M. (1990) *Pharmacol. Ther. 46*, 297−311.

Modi, S., Primrose, W. U., Boyle, J., Gibson, C. F., Lian L.-Y., & Roberts, G. C. K. (1995a) *Biochemistry 34*, 8982−8988.

Modi, S., Primrose, W. U., Lian, L.-Y., & Roberts, G. C. K. (1995b) *Biochem. J. 310*, 939−943.

Mortimer, O., Persson, K., Ladona, M. G., Spalding, D., Zanger, U. M., Meyer, U. A., & Rane, A. (1990) *Clin. Pharmacol. Ther. 47*, 27−35.

Omura, T., & Sato, R. (1964) *J. Biol. Chem. 239*, 2379−2387.

O'Reilly, D. R., Brown, M. R., & Miller, L. K. (1992) *Insect Biochem. Mol. Biol. 22*, 313−320.

Paine, M. J. I., Gilham, D., Roberts, G. C. K., & Wolf, C. R. (1996) *Arch. Biochem. Biophys.* (in press).

Penman, B. W., Reece, J, Smith, T., Yang, C. S., Gelboin, H. V., Gonzalez, F. J., & Crespi, C. L. (1993) *Pharmacogenetics 3*, 28−39.

Philson, S. B., Debrunner, P. G., Schimidt, P. G., & Gunsalus, I. C. (1979) *J. Biol. Chem. 254*, 10173−10179.

Poulos, T. L., & Raag, R. (1992) *FASEB J. 6*, 674−679.

Poulos, T. L., Finzel, B. C., & Howard, A. J. (1986) *Biochemistry 25*, 5314−5321.

Poulos, T. L., Finzel, B. C., & Howard, A. J. (1987) *J. Mol. Biol. 195*, 687−700.

Raag, R., Martinis, S. A., Sligar, S. G., & Poulos, T. L. (1991) *Biochemistry 30*, 11420−11429.

Raag, R., Li, H., Jones, B. C., & Poulos, T. L. (1993) *Biochemistry 32*, 4571−4578.

Ravichandran, K. G., Boddupalli, S. S., Hasemann, C. A., Peterson, J. A., & Deisenhofer, J. (1993) *Science 261*, 731−735.

Sali, A., & Blundell, T. L. (1993) *J. Mol. Biol. 234*, 779−815.

Sariaslani, F. S. (1991) *Adv. Appl. Mirobiol. 36*, 133−178.

Shiro, Y., Iizuka, T., Makino, R., Ishimura, Y., & Morishima, I. (1989) *J. Am. Chem. Soc. 111*, 7707−7712.

Solomon, I., & Bloembergen, N. (1956) *J. Chem. Phys. 25*, 261.

Woldman, Ya.Yu., Weiner, L. M., Gulyaeva, L. F., & Lyakhovich, V. V. (1985) *FEBS Lett. 181*, 295−299.

Wolff, T., Distlerath, L. M., Worthington, M. T., Groopman, J. D., Hammons, G. J., Kadlubar, F. F., Prough, R. A., Martin, M. V., & Guengerich, F. P. (1985) *Cancer Res. 45*, 2116−2122.

Zvelebil, M. J. J. M., Wolf, C. R., & Sternberg, M. J. E. (1991) *Protein Eng. 4*, 271−282.

BI952742O